

# Quantitative Analysis of Acute Myocardial Infarct in Rat Hearts with Ischemia–Reperfusion Using a High-Resolution Stationary SPECT System

Zhonglin Liu, MD; George A. Kastis, MS; Gail D. Stevenson, DVM; Harrison H. Barrett, PhD; Lars R. Furenlid, PhD; Matthew A. Kupinski, PhD; Dennis D. Patton, MD; and Donald W. Wilson, PhD

Department of Radiology, University of Arizona Health Sciences Center, Tucson, Arizona

The purpose of this study was to develop an *in vivo* imaging protocol for a high-resolution stationary SPECT system, called FASTSPECT, in a rat heart model of ischemia–reperfusion (IR) and to compare  $^{99m}\text{Tc}$ -sestamibi imaging and triphenyltetrazolium chloride (TTC) staining for reliability and accuracy in the measurement of myocardial infarcts. **Methods:** FASTSPECT consists of 24 modular cameras and a 24-pin-hole aperture with 1.5-mm spatial resolution and 13.3 cps/ $\mu\text{Ci}$  (0.359 cps/kBq) sensitivity. The IR heart model was created by ligating the left coronary artery for 90 min and then releasing the ligature for 30 min. Two hours after  $^{99m}\text{Tc}$ -sestamibi injection (5–10 mCi [185–370 MBq]), images were acquired for 5–10 min for 5 control rats and 11 IR rats. The hearts were excised, and the left ventricle was sectioned into 4 slices for TTC staining. **Results:** Left and right ventricular myocardium in control rats was shown clearly, with uniform  $^{99m}\text{Tc}$ -sestamibi distribution and 100% TTC staining for viable myocardium. Nine of 11 rats with IR survived throughout imaging and exhibited  $50.8\% \pm 2.7\%$  ischemic area and  $37.9\% \pm 3.9\%$  infarct in the left ventricle on TTC staining. The infarct size measured by FASTSPECT imaging was  $37.6\% \pm 3.6\%$ , which correlated significantly with that measured by TTC staining ( $r = 0.974$ ;  $P < 0.01$ ). **Conclusion:** The results confirmed the accuracy of FASTSPECT imaging for measurement of acute myocardial infarcts in rat hearts. Application of FASTSPECT imaging in small animals may be feasible for investigating myocardial IR injury and the effects of revascularization.

**Key Words:** high-resolution SPECT;  $^{99m}\text{Tc}$ -sestamibi; myocardial infarction; ischemia–reperfusion

**J Nucl Med 2002; 43:933–939**

**L**arge animals such as dogs are often used for *in vivo* experimental imaging of coronary artery disease. However, large animals are expensive, and experience with surgical

techniques is required. Development of novel myocardial imaging techniques and preclinical testing of cardiovascular radiopharmaceuticals require an *in vivo* heart model of small animals such as rats. In recent years, high-resolution tomographic imaging has become available for small-animal studies in basic biomedical science or preclinical research studies (1). High-resolution SPECT systems (2–5) have been found useful in myocardial imaging, functional brain imaging, and gene-expression studies. The Radiology Research Laboratory at the University of Arizona (Tucson, AZ) has designed and built a high-spatial-resolution SPECT system, called FASTSPECT, that consists of 24 modular cameras with a multiple-pin-hole aperture (6). The FASTSPECT system was originally designed as a brain imager. Using a 24-pin-hole cylindrical aperture, FASTSPECT can be applied to small-animal cardiac imaging.

Interest has been growing in the use of SPECT to determine myocardial infarct size (7–9). Measurement of the acute myocardial perfusion defect by injection of perfusion agents, such as  $^{99m}\text{Tc}$ -sestamibi, during coronary occlusion indicates the amount of myocardium at risk. Injection of  $^{99m}\text{Tc}$ -sestamibi after coronary reperfusion permits measurement of infarct size. When obtained through high-resolution imaging of small animals, these measurements can be used to investigate metabolism, revascularization therapy, gene therapy, novel cardiovascular medicines for salvaging myocardium that has undergone ischemia–reperfusion (IR), and new radiopharmaceuticals for diagnosing myocardial ischemia and infarction.

The purpose of this study was to develop an *in vivo* imaging protocol for FASTSPECT in a rat model of myocardial IR and to compare  $^{99m}\text{Tc}$ -sestamibi imaging and triphenyltetrazolium chloride (TTC) staining for reliability and accuracy in the measurement of myocardial infarct size.

## MATERIALS AND METHODS

### Animal Preparation and IR Heart Model

Sixteen male Sprague–Dawley rats (body weight range, 250–350 g) were used in the experiments and were separated into 2

Received Oct. 9, 2001; revision accepted Mar. 25, 2002.  
For correspondence or reprints contact: Zhonglin Liu, MD, Department of Radiology, University of Arizona Health Sciences Center, P.O. Box 245067, Tucson, AZ 85724-5067.  
E-Mail: zliu@radiology.arizona.edu

groups. Normal myocardial imaging with  $^{99m}\text{Tc}$ -sestamibi was performed without surgery on 5 rats, which served as a control group. An additional 11 rats served as an IR group to undergo  $^{99m}\text{Tc}$ -sestamibi imaging. The rats were anesthetized with pentobarbital (40 mg/kg). Additional anesthesia was given during the experiment as necessary.

The rats in the IR group were prepared by removing the fur from the chest and neck with electric clippers. After tracheotomy, the rats were ventilated by a volume-controlled Inspira Advanced Safety Ventilator (Harvard Apparatus, Inc., Holliston, MA) with a mixture of oxygen and room air. Using each animal's weight, Safe Range software (Harvard Apparatus) automatically calculated the correct tidal volume (1.5–2.1 mL) and respiration rate (70–77 breaths per minute) for that animal. The heart was exposed through a left thoracotomy incision. Myocardial IR was produced by a technique similar to techniques described previously (10–11). A small, curved, tapered needle carried a 5-0 silk thread through the tissue between the pulmonary cone and the left auricular appendage. The ligature was tied around the left coronary artery (LCA) with a small bundle of myocardium. The LCA was occluded for 90 min using a temporary ligature (12). Thirty minutes of reperfusion were achieved by release of the ligature.

### FASTSPECT System

The FASTSPECT system (6) has 24 small, modular gamma cameras arranged in 2 circular arrays: 1 array of 11 cameras and 1 array of 13 cameras. Each modular camera consists of a  $10 \times 10$  cm NaI(Tl) scintillation crystal (Rexon Components, Inc., Beachwood, OH), an optical light guide, 4 square ( $5 \times 5$  cm) photomultiplier tubes (Hamamatsu Photonics K.K., Hamamatsu, Japan), and associated electronics. The unshrouded system is shown in Figure 1. Twenty-four 1-mm-diameter pinholes were drilled in a cylindrical aperture such that a point source in the center of the field of view was simultaneously projected to the center of each camera. The total magnification was 3.5 in a  $3.0 \times 3.2 \times 3.2$  cm field of view. The sensitivity of the system for a point source in air was 13.3 cps/ $\mu\text{Ci}$  (0.359 cps/kBq). The system response matrix  $H$  was measured by moving a 1-mm point source in incremental steps inside the object space.

### Image Acquisition

$^{99m}\text{Tc}$ -sestamibi (5–10 mCi [185–370 MBq]) was injected through the femoral vein of both control and IR rats after 30 min of reperfusion. Each rat was placed into the aperture using a 6-cm-diameter cylindrical cardboard holder, which was mounted on a translation stage for accurate positioning of the heart in the center of the field of view. Multiple images were acquired for 5–10 min from 1 to 2 h after a  $^{99m}\text{Tc}$ -sestamibi injection. Twenty-four projections were obtained, 1 from each camera. Projection images were generated using a lookup-table scheme. In this scheme, each scintillation event within the NaI crystal of the camera was registered as the digitized output from the 4 photomultiplier tubes of the camera. To estimate energy and interaction position, the 4 outputs were then compared with a 20-bit lookup table. This table was precalculated using a calibration procedure that involved moving a collimated source across the camera face. The projections were transferred to a workstation, where a 3-dimensional image was obtained using 100 iterations of the maximum-likelihood expectation maximization (MLEM) reconstruction algorithm (13–15). Spatial resolution in the reconstructed image was approximately 1.5 mm in all 3 directions.

### Myocardial Ischemic Area at Risk and TTC Infarct Size Measurement

After the heart had been imaged, the LCA with IR was reoccluded. Evans blue dye (1.5%, 1.0 mL) in phosphate-buffered saline (PBS) was injected into the left ventricular cavity to measure the myocardial ischemic area at risk. The animal was killed by a pentobarbital overdose. For both the control group and the IR group, the entire heart was excised and weighed. The  $^{99m}\text{Tc}$  activity in the heart was measured in a dose calibrator. The great vessels, atria, and right ventricle of the heart were removed. The left ventricle was sectioned into 4 transverse slices in a plane parallel to the atrioventricular groove. Both sides of the tissue slices were immediately photographed using a digital camera (D-500L; Olympus Optical Co., Ltd., Tokyo, Japan).

TTC staining was used to assess myocardial tissue viability and determine myocardial infarct size. The tissue slices were incubated in 1% TTC PBS solution, pH 7.4, at 37°C for 20 min. Tissues were

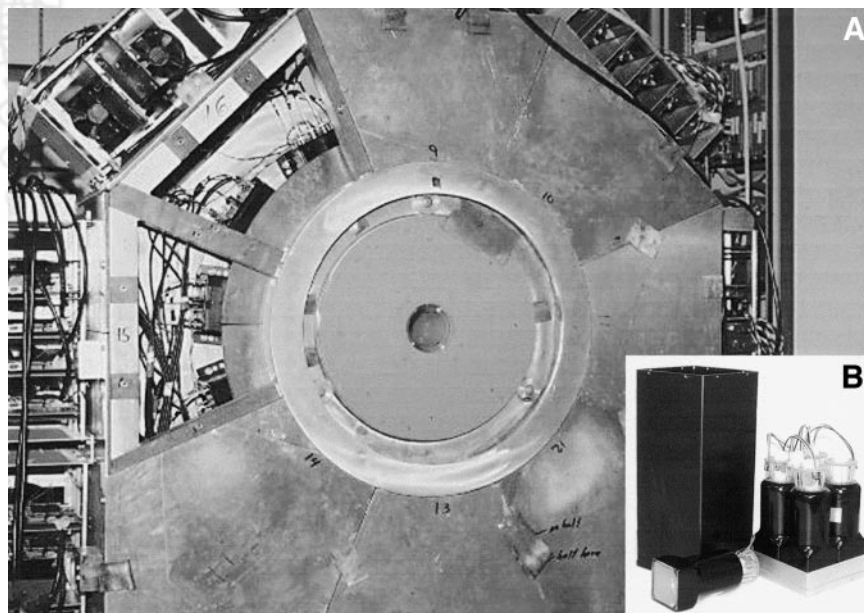


**FIGURE 1.** (A) High-resolution stationary SPECT system, FASTSPECT. Four modular cameras can be seen through window, where 2 sheets of lead were removed. (B) Photomultiplier tube (Hamamatsu Photonics K.K., Hamamatsu, Japan) and modular scintillation camera of FASTSPECT system.

fixed in 10% PBS-buffered formalin overnight at 2°C–8°C. Both sides of each TTC-stained tissue slice were photographed with the digital camera.

The digital photographs were downloaded to a personal computer. The ischemic area at risk (unstained by Evans blue dye) and the infarcted area (unstained by TTC) were measured using SigmaScan software (SPSS Science, Chicago, IL) in trace-measurement mode. That mode was used to measure either the ischemic area or the infarcted area, which is a sum of calibrated pixels in a defined region, through manually drawing an image layer on the photograph. The results appeared in the specified worksheet columns as the measurements were made. Infarct size was expressed both as a percentage of total left ventricular mass and as a percentage of the ischemic area at risk. The correlation between photographs of TTC staining and FASTSPECT images 2 h after MIBI injection with respect to infarct size was analyzed.

### Image Processing

Tomographic reconstruction was performed using the MLEM algorithm. The projection model built into this algorithm was generated using a calibration scheme that involved moving an uncollimated source through the imaging field of view of the system and recording its response at each calibration point. With Slicer Dicer software (Pixotec, LLC, Renton, WA), the transaxial data were reoriented obliquely, and long- and short-axis slices of the heart were generated with a 1-pixel thickness (1.0 mm). A lower threshold value was set at approximately 60 in a color range from 0 to 255 to display methoxyisobutylisonitrile myocardial uptake.

The defect of  $^{99m}\text{Tc}$ -sestamibi myocardial distribution in each short-axis slice was quantified on the images 2 h after injection using the trace-measurement mode of the SigmaScan software. The radioactive defects of short-axis slices were averaged as a percentage of the entire left ventricle.

### Data Analysis

All results are expressed as mean  $\pm$  SEM. Groups were compared using 1-way ANOVA. Variables within a group were compared using a paired  $t$  test. Probability values  $< 0.05$  were considered significant. The correlation between  $^{99m}\text{Tc}$ -sestamibi-measured myocardial defects and TTC-measured myocardial infarct size was assessed using linear regression analysis.

### Ethics

All experiments were performed in accordance with the animal research guidelines of the National Institutes of Health (16) and were approved by the Institutional Animal Care and Use Committee of the University of Arizona.

## RESULTS

### Normal Myocardial Images

All rats in the control group survived throughout image acquisition. In the short-axis images, vertical and horizontal long-axis images, and 3-dimensional displays, left ventricular myocardium and right ventricular myocardium were shown clearly, with uniform distribution of  $^{99m}\text{Tc}$ -sestamibi in all images. The representative images of 1 control rat heart are shown in Figure 2. TTC staining showed that all myocardial regions were 100% viable (Fig. 3).

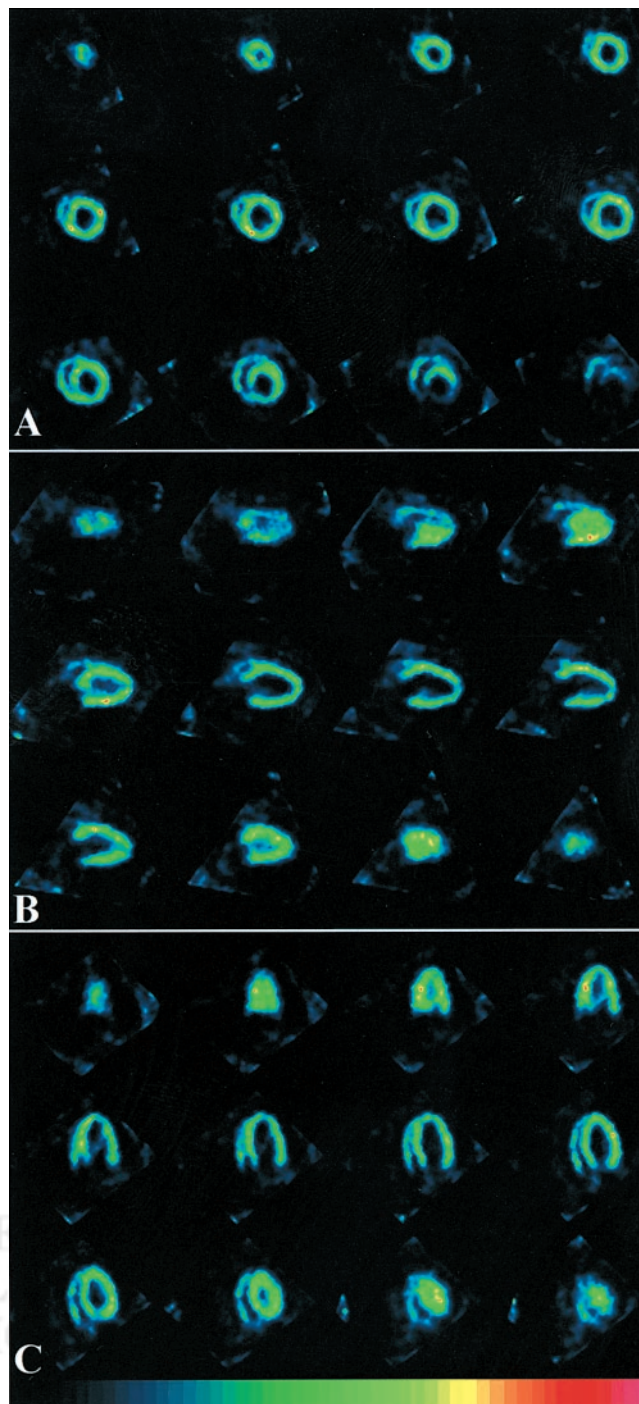


**FIGURE 2.** Representative  $^{99m}\text{Tc}$ -sestamibi tomograms from 1 control rat heart 2 h after injection, including short-axis (A), vertical long-axis (B), and horizontal long-axis (C) views.

### Images of Myocardium with IR

In the IR group, 1 rat died 10 min after reperfusion and 1 rat died 30 min after  $^{99m}\text{Tc}$ -sestamibi injection. The FASTSPECT images of the 9 surviving rats showed regional defects localized in the LCA-supplied area, including the anterior wall, apex, and part of the lateral wall of the left ventricle (Fig. 4). The right ventricular myocardium was

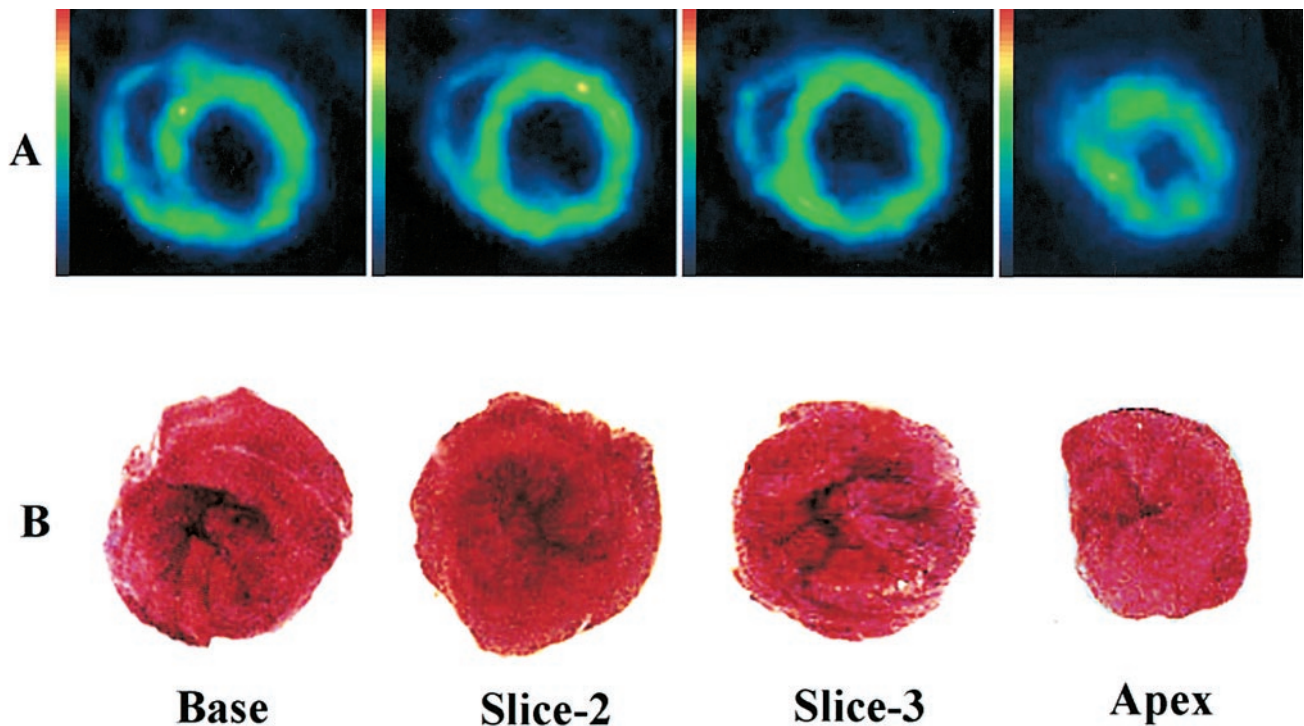


**FIGURE 3.** (A) FASTSPECT imaging shows uniform myocardial distribution of  $^{99m}\text{Tc}$ -sestamibi in control rat heart. (B) Left ventricular myocardium in control rat heart was stained red by TTC and exhibits 100% viability. Differences in cavity size and left ventricular wall thickness are caused by postmortem shrinking of tissue.

fully visible for all 9 IR rats, with uniform  $^{99m}\text{Tc}$ -sestamibi distribution.

#### Myocardial Ischemic Area at Risk and Infarct Size

In the 9 surviving rats of the IR group, TTC staining showed myocardial infarction. The myocardial ischemic area at risk, as determined by lack of Evans blue dye, was  $50.8\% \pm 2.7\%$  in those rats. The  $^{99m}\text{Tc}$ -sestamibi defects on FASTSPECT images were consistent with the unstained areas on TTC staining (Fig. 5). For the left ventricle, the infarct size measured by TTC staining was  $37.9\% \pm 3.9\%$ , which was  $73.0\% \pm 4.9\%$  of the ischemic area at risk. The infarct size measured by FASTSPECT imaging was  $37.6\% \pm 3.6\%$ , which was  $72.9\% \pm 4.4\%$  of the ischemic area at risk. No significant difference was found between the infarct size measured by TTC staining and the infarct size measured by FASTSPECT imaging ( $P > 0.05$ ). Figure 6 shows a significant correlation between infarct size on TTC staining and infarct size on FASTSPECT imaging ( $r = 0.974$ ;  $P < 0.01$ ).

#### DISCUSSION

In this study, an in vivo IR rat heart model was developed.  $^{99m}\text{Tc}$ -sestamibi in vivo imaging was performed on normal myocardium and myocardium with acute infarction using a high-resolution stationary SPECT system, FASTSPECT. The acquisition procedures, imaging process, and reconstruction in the rat heart model were programmed. Infarct

measurement through imaging was evaluated and compared with that through myocardial TTC staining.

Higher-resolution small-animal imaging systems using SPECT (2–6,17,18) and PET (19,20) are continuously being sought and developed to improve spatial detail and image quality in basic biomedical science or preclinical research studies. Pinhole planar imaging may be adequate for small-animal imaging in some studies but is not adequate in studies that require accurate quantitative analysis of images.

FASTSPECT has unique advantages. The system was originally designed and built for human brain imaging. By adopting a cylindrical aperture with 24 pinholes 1 mm in diameter, FASTSPECT can be used for imaging small animals such as rats and mice. The name *FASTSPECT* (Fast Stationary SPECT) was chosen because no motion by the aperture or detector is required for acquisition of projection data. Artifacts caused by detector motion or aperture structure are therefore avoided. FASTSPECT is a true dedicated 4-dimensional imaging system with stationary camera modules and a stationary multiple-pinhole aperture (6,18).

$^{99m}\text{Tc}$ -sestamibi has been widely used as a perfusion imaging agent in the diagnosis of coronary artery disease. Experimental and clinical studies have suggested that  $^{99m}\text{Tc}$ -sestamibi is useful in the evaluation of myocardial viability (21–25). In myocardium with IR, irreversible myocardial damage occurs when the ischemia is severe and prolonged.

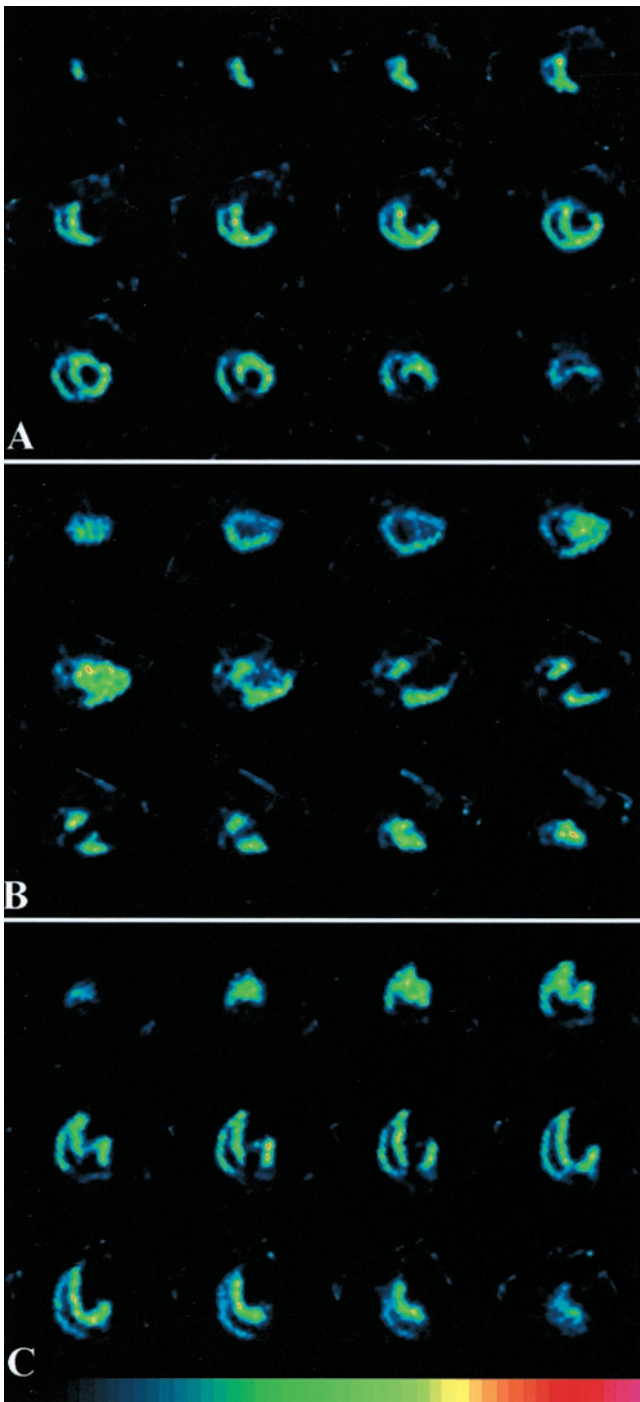


**FIGURE 4.** Representative  $^{99m}\text{Tc}$ -sestamibi images from 1 IR rat heart 2 h after injection, including short-axis (A), vertical long-axis (B), and horizontal long-axis (C) views. Regional perfusion defects are localized in anterior wall, apex, and part of lateral wall of left ventricle.

$^{99m}\text{Tc}$ -sestamibi cannot be retained in myocardial regions that have been irreversibly injured by prolonged coronary occlusion followed by reperfusion (26). Thus,  $^{99m}\text{Tc}$ -sestamibi imaging is valuable for assessing both the myocardium at risk and the infarct.  $^{99m}\text{Tc}$ -sestamibi myocardial activity correlates with the amount of viable myocardium stained by

TTC (25). Absence of TTC staining indicates myocardial enzyme release and membrane damage in the nonviable myocardium. The extent of the left ventricular perfusion defect on  $^{99m}\text{Tc}$ -sestamibi images reflects the size of the myocardial infarction (23,27).

Using rotating-pinhole SPECT cameras, studies have shown that myocardial infarcts can be detected and quantitatively measured in rat heart models (4,28). In those reported studies, myocardial infarcts were determined 48 h after LCA occlusion with reperfusion (4) and 24 d after occlusion without reperfusion (25). Because rotating SPECT cameras were used, 30–60 min of acquisition time were required. In this study, we developed an acute IR rat heart model that more closely relates to clinical cases of acute heart attack and revascularization. The IR in the rat heart model was applied by temporary ligation of the LCA, and acute myocardial infarction was successfully induced. Using FASTSPECT, high-quality images were achieved using only 5- to 10-min acquisitions 1–2 h after  $^{99m}\text{Tc}$ -sestamibi injection. Both the left and the right ventricles were displayed fully and clearly. The myocardial defects of  $^{99m}\text{Tc}$ -sestamibi activity seen on FASTSPECT images of the hearts with acute IR were consistent with the myocardial infarcts seen on photographs of TTC staining. An excellent correlation was shown between infarct sizes measured on FASTSPECT imaging and those measured through TTC staining.

In small-animal models of acute myocardial infarction, the duration of anesthesia and the intravenously injected volume of imaging agent are limited. Fast, repeated imaging combining high sensitivity and high spatial resolution is required so that the ongoing myocardial injury produced by IR can be detected effectively and repeatedly. Using FASTSPECT, a rapid sequence of 3-dimensional images can be acquired in the rat heart model. For tomographic imaging, no uniformity or center-of-rotation corrections are required, and an artifact caused by an inaccurate rotation center is not present. Scatter influence from neighboring organs is minimal in this imaging system, so we did not use any shielding, such as an abdominal lead belt.

In this open-chest rat heart model with acute IR, hemodynamic measurement was not applied. The hemodynamic status may not be consistent among experimental animals. In addition, when the infarcted myocardium involves a large defect with  $^{99m}\text{Tc}$ -sestamibi, there may be an invisible outline of myocardial activity in the apex, complicating quantitative analysis using the SigmaScan planimetry measurement. The analysis of short-axis circumferential profiles may allow more accurate identification of the infarct zone. Gating SPECT provides a valuable adjunct in characterizing fixed defects and enhancing the assessment of myocardial viability with  $^{99m}\text{Tc}$ -sestamibi. Gated tomographic imaging is not available in the current version of FASTSPECT but will be available in a new system, FASTSPECT II, which will soon be online.

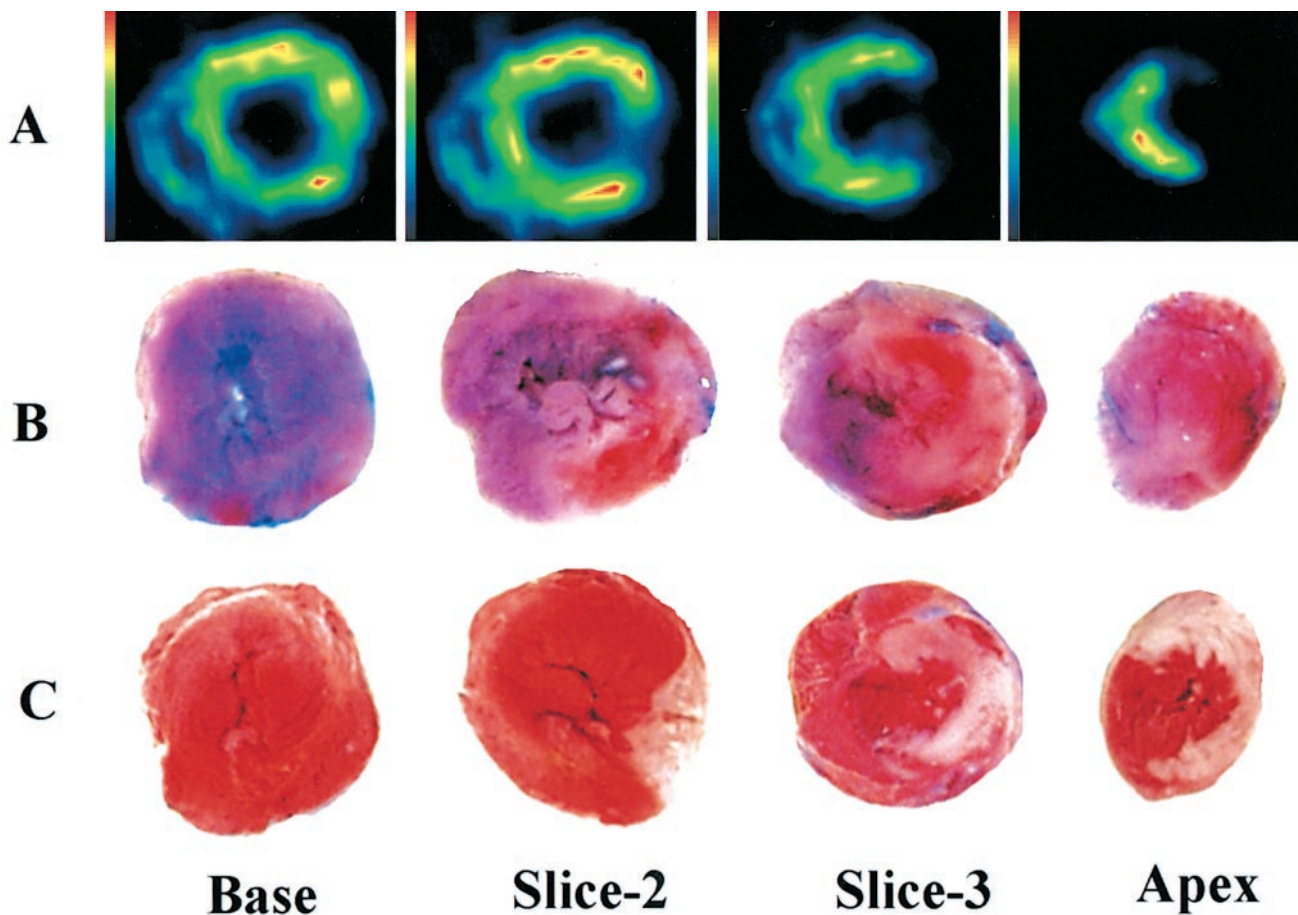


**FIGURE 5.** Perfusion defects seen on FASTSPECT  $^{99m}\text{Tc}$ -sestamibi images 2 h after injection in heart with IR (A) are consistent with myocardial ischemic area at risk, as determined by Evans blue dye (unstained by blue dye) (B), and with infarct myocardium, as determined by TTC staining (unstained by TTC) (C).

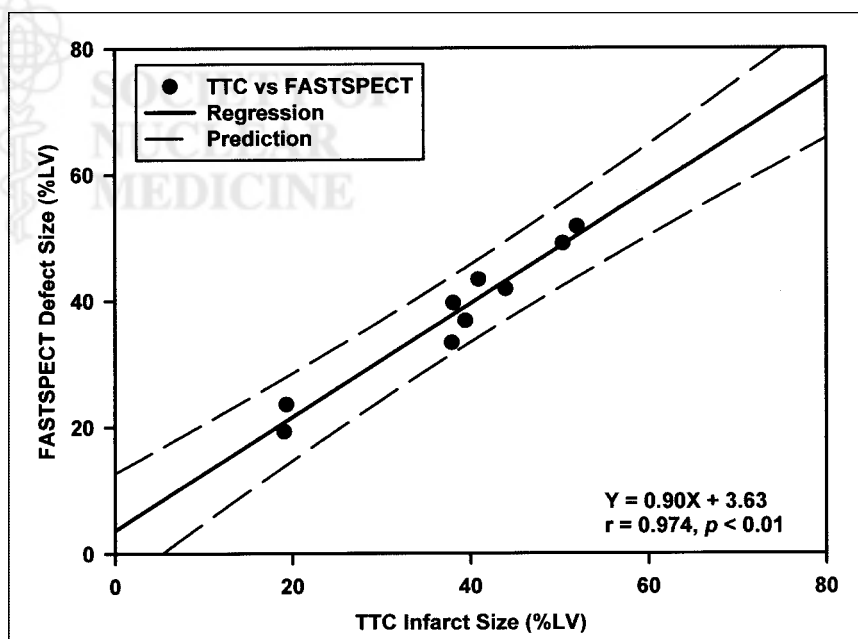


**FIGURE 6.** Scatterplot shows correlation between  $^{99m}\text{Tc}$ -sestamibi radioactive defect size on FASTSPECT images 2 h after injection and anatomic infarct size (TTC staining). LV = left ventricle.

## CONCLUSION

A successful myocardial IR rat model was developed, and acute myocardial infarct size was accurately measured using FASTSPECT imaging. This study showed that application of FASTSPECT imaging in small animals may be feasible for investigating myocardial IR injury and the effects of revascularization.

## ACKNOWLEDGMENTS

The authors acknowledge the secretarial assistance of Jane Lockwood and Lisa Gelia. This study was supported by grants 5P41RR14304 and R24CA83148 from the National Institutes of Health.

## REFERENCES

1. Weber DA, Ivanovic M. Ultra-high-resolution imaging of small animals: implications for preclinical and research studies. *J Nucl Cardiol*. 1999;6:332–344.
2. Weber DA, Ivanovic M, Franceschi D, et al. Pinhole SPECT: a new approach to in vivo high resolution SPECT imaging in small laboratory animals. *J Nucl Med*. 1994;35:342–348.
3. Ishizu K, Mukai T, Yonekura Y, et al. Ultra-high resolution SPECT system using four pinhole collimators for small animal studies. *J Nucl Med*. 1995;36:2282–2287.
4. Yukihiko M, Inoue T, Iwasaki T, Tomiyoshi K, Erlandsson K, Endo K. Myocardial infarction in rats: high-resolution single-photon emission tomographic imaging with a pinhole collimator. *Eur J Nucl Med*. 1996;23:896–900.
5. Weisenberger AG, Bradley E, Majewski S, Saha M. Development of a novel radiation imaging detector system for in vivo gene imaging in small animals studies. *IEEE Trans Nucl Sci*. 1998;45:1743–1749.
6. Klein WP, Barrett HH, Pang IW, et al. FASTSPECT: electrical and mechanical design of a high-resolution dynamic SPECT imager. In: *Conference Record of the 1995 IEEE Nuclear Science Symposium and Medical Imaging, San Francisco, CA*. Vol 2. Los Alamitos, CA: IEEE; 1995:931–933.
7. O'Connor MK, Gibbons RJ, Juni JE, O'Keefe J Jr, Ali A. Quantitative myocardial SPECT for infarct sizing: feasibility of a multicenter trial evaluated using a cardiac phantom. *J Nucl Med*. 1995;36:1130–1136.
8. Kang X, Berman DS, Van Train KF, et al. Clinical validation of automatic quantitative defect size in rest technetium-99m-sestamibi myocardial perfusion SPECT. *J Nucl Med*. 1997;38:1441–1446.
9. Gibbons RJ, Miller TD, Christian TF. Infarct size measured by single photon emission computed tomographic imaging with (99m)Tc-sestamibi: a measure of the efficacy of therapy in acute myocardial infarction. *Circulation*. 2000;101:101–108.
10. Kaufman N, Gavan TL, Hill RW. Experimental myocardial infarction in the rat. *Arch Pathol*. 1959;67:482–488.
11. Selye H, Bajusz E, Grasso S, Mendell P. Simple techniques for the surgical occlusion of coronary vessels in the rat. *Angiology*. 1960;11:398–403.
12. Deloche A, Fabiani JN, Camilleri JP, et al. The effect of coronary artery reperfusion on the extent of myocardial infarction. *Am Heart J*. 1977;93:358–366.
13. Shepp LA, Vardi Y. Maximum likelihood reconstruction for emission tomography. *IEEE Trans Med Image*. 1982;1:113–122.
14. Lange K, Carson. EM reconstruction algorithms for emission and transmission tomography. *J Comput Assist Tomogr*. 1984;8:306–316.
15. Beekman FJ, Kamphuis C, Frey E. Scatter compensation methods in 3D iterative SPECT reconstruction? A simulation study. *Phys Med Biol*. 1997;42:1619–1632.
16. National Research Council. *Guide for the Care and Use of Laboratory Animals*. Bethesda, MD: United States Department of Health and Human Services, National Institutes of Health; 1985. NIH publication 85-23.
17. Smith MF, Jaszczak RJ. An analytic model of pinhole aperture penetration for 3D pinhole SPECT image reconstruction. *Phys Med Biol*. 1998;43:761–775.
18. Katis GK, Barber HB, Barrett HH, et al. High resolution SPECT imager for three-dimensional imaging of small animals [abstract]. *J Nucl Med*. 1998;39(suppl):9P.
19. Cherry SR, Shao Y, Silverman RW, et al. High resolution PET scanner for imaging small animals. *IEEE Trans Nucl Sci*. 1997;44:1161–1166.
20. Bloomfield PM, Rajeswaran S, Spinks TJ, et al. The design and physical characteristics of a small animal positron emission tomograph. *Phys Med Biol*. 1995;40:1105–1126.
21. Crane P, Laliberte R, Heminway S, Thoolen M, Orlandi C. Effect of mitochondrial viability and metabolism on technetium-99m-sestamibi myocardial retention. *Eur J Nucl Med*. 1993;20:20–25.
22. Kauffman GJ, Boyne TS, Watson DD, Smith WH, Beller GA. Comparison of rest thallium-201 imaging and rest technetium-99m sestamibi imaging for assessment of myocardial viability in patients with coronary artery disease and severe left ventricular dysfunction. *J Am Coll Cardiol*. 1996;27:1592–1597.
23. Sinusas AJ, Trautman KA, Bergin JD, et al. Quantification of area at risk during coronary occlusion and degree of myocardial salvage after reperfusion with technetium-99m methoxyisobutyl isonitrile. *Circulation*. 1990;82:1424–1437.
24. vom Dahl J, Althoefer C, Sheehan FH, et al. Effect of myocardial viability assessed by technetium-99m-sestamibi SPECT and fluorine-18-FDG PET on clinical outcome in coronary artery disease. *J Nucl Med*. 1997;38:742–748.
25. Liu Z, Johnson G III, Beju D, Okada RD. Detection of myocardial viability in ischemic-reperfused rat hearts by <sup>99m</sup>Tc-sestamibi kinetics. *J Nucl Cardiol*. 2001;8:677–686.
26. Leon AR, Eisner RL, Martin SE, et al. Comparison of single-photon emission computed tomography (SPECT) myocardial perfusion imaging with thallium-201 and technetium-99m sestamibi in dogs. *J Am Coll Cardiol*. 1992;20:1612–1625.
27. Verani MS, Jeroudi MO, Mahmarian JJ, Boyce TM, Borges-Neto S, Patel F. Quantification of myocardial infarction during coronary occlusion and myocardial salvage after reperfusion using cardiac imaging with technetium-hexakis 2-methoxyisobutyl isonitrile. *J Am Coll Cardiol*. 1988;12:1573–1581.
28. Hirai T, Nohara R, Hosokawa R, et al. Evaluation of myocardial infarct size in rat heart by pinhole SPECT. *J Nucl Cardiol*. 2000;7:107–111.

